Magnetic reconnection in solar flares and pulsar magnetospheres

Don Melrose

SIfA, School of Physics
University of Sydney

July 12, 2016

Outline

- Early history of reconnection
- 2D models for reconnection
- Enhanced reconnection
- 3D flare models
- Currents in solar flares
- Magnetic helicity
- Reconnection in 3D
- Summary and conclusions
- Reconnection in a pulsar magnetosphere

Many of the ideas on solar flares are described by cartoons, see Hudson's Solar cartoon archive:
`http://solarmuri.ssl.berkeley.edu/~hhudson/cartoons/`

In this talk I will follow the development of important ideas using cartoons, for both solar flare and geomagnetic substorms.

Early history of reconnection: solar flares

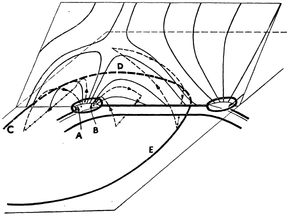

Fig. 1.—*Currents near a growing bipolar spot group.*

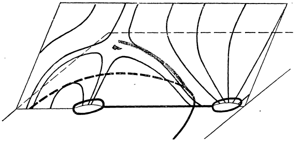

Fig. 2.—*Neutral point flare.*

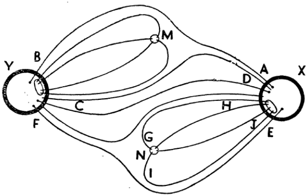

Giovanelli's (1946, 1947, 1948) cartoons for "chromospheric flares" describing currents, magnetic nulls and a quadrupolar magnetic structure, respectively.

2D models: Dungey (1953)

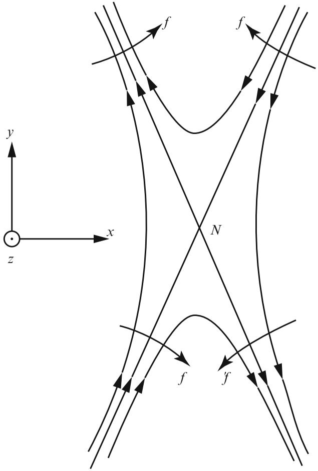

Dungey (*Phil. Mag.* 44, 725, 1953) initiated the development of reconnection models. The figure is from Dungey's (1958) book. The curved arrows labeled f indicate the direction of plasma flow. Individual magnetic field lines flow with the plasma. The overall pattern does not change with time.

Model is an X-type neutral point.

Magnetic reconnection is an intrinsically time-dependent problem, and must involve an inductive electric field.
All reconnection model are time-independent.

2D models: Sweet-Parker

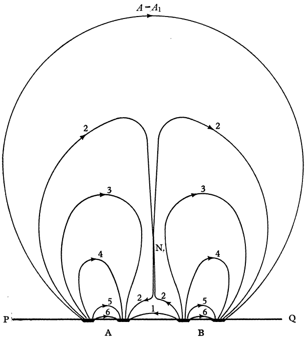

Fig. 3. Field of displaced systems in perfectly conducting medium.

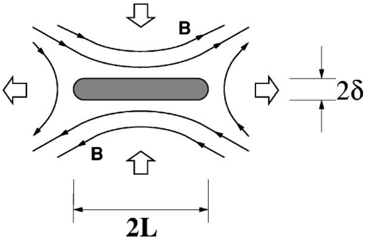

Left: Sweet (1958) presented a "neutral point theory for solar flares"; cartoon shows extended vertical neutral point/plane.
Right: In the Sweet-Parker model reconnection occurs in a current sheet. Reconnection occurs by oppositely directed magnetic field lines diffusing together and annihilating.
For $L \gg \delta$ reconnection is far too slow to explain a solar flare.

2D models: Petschek

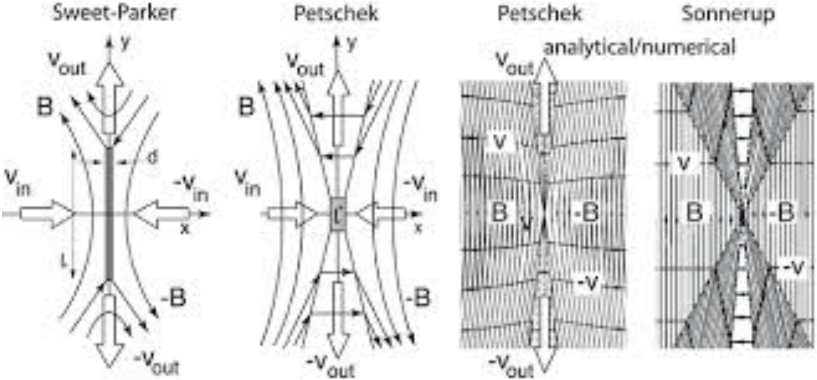

Petschek's (1964) model allows much faster reconnection. Reconnection is confined to a tiny region, and the reconnected field and plasma are transported away by slow-mode shocks.

2D models: tearing instability

In laboratory plasma physics it was recognized that a current sheet with finite conductivity is unstable to a tearing mode.

(Furth, Killeen & Rosenbluth: 1963, *Phys. Fluids*, 6, 459, 1963)

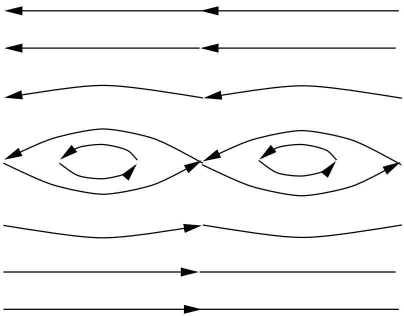

The current (flowing perpendicular to the page) in a sheet breaks up into current lines, along the centers of the magnetic bubbles.

2D models: "standard" flare model

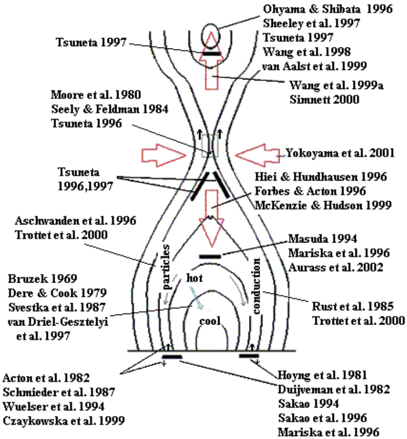

Version of CSHKP model for a solar flare (McKenzie 2002).
Reconnection occurs in a current sheet similar to Sweet (1958).

Early history of reconnection: open magnetosphere

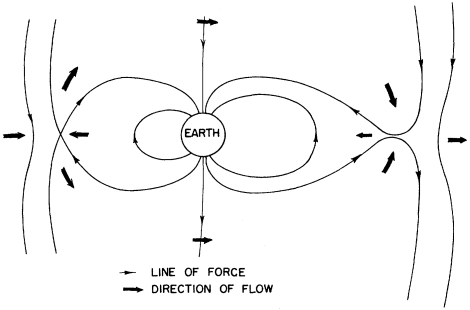

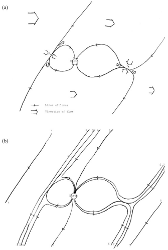

Dungey (PRL **6**, 47) (1961) presented a model for the magnetosphere with reconnection between the Earth's magnetic field and the interplanetary magnetic field at two points. This model already appeared in Dungey's PhD thesis in 1950.

2D models: dipolarization in the magnetotail

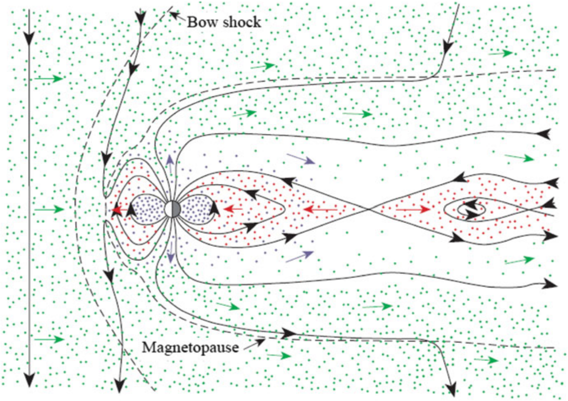

Fig. 1.8 Noon-midnight meridian cross-section through the Earth's magnetosphere, where the *arrowed solid lines* show magnetic field lines, while the *dashed lines* show the bow shock and magnetopause as marked. The *coloured dots* show the principal plasma populations originating in the solar wind (*green*) and the Earth's ionosphere (*blue*). Both sources contribute to the hot plasma sheet population located at the centre plane of the tail (*red*). From Cowley et al. (2003) (Color figure online)

Version of standard model for reconnection in the Earth's magnetotail (Cowley 2015).

Enhanced reconnection: anomalous resistivity

The rate of reconnection can be greatly enhanced by appealing to anomalous conductivity. (Kulsrud, *Earth Planets Space*, **53**, 417, 2001)

Anomalous conductivity is attributed to a current driven (kinetic) instability that generates longitudinal waves; these waves scatter the current-carrying electrons, impeding the flow of current.

The anomalously conducting region is confined to a tiny volume compared with the volume of flaring region—ratio of scale lengths of order 10^{-6}.

Kulsrud (2001) argued that both Sweet-Parker and Petschek reconnections are enhanced when anomalous conductivity is assumed uniform, and that Petschek reconnection is strongly favored for (as expected) localized anomalous conductivity.

Enhanced reconnection: turbulence

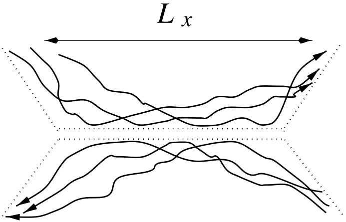

(Lazarian & Vishniac, ApJ, **517**, 700, 1999)

By adding MHD turbulence to a Sweet-Parker model, the smooth current sheet develops a large number of magnetic nulls. This results in turbulent reconnection.

A weakness in existing models for reconnection is their tiny scale compared with scales relevant to a solar flare. A statistically large number of reconnection sites, operating simultaneously and coupled together, is needed to explain effective reconnection on a large scale. Turbulent reconnection is one way of achieving this.
(Lazarian *et al.*, *Phil. Trans. Roy. Soc.* **373**, 20140144, 1999; Huang & Bhattacharjee, ApJ, **818**, 20, 2016).

3D flare models: sheared arcade

Realistic flare models require 3D reconnection. Two classes of 3D flare model are a sheared magnetic arcade, and a quadrupolar model involving a newly emerging flux tube.

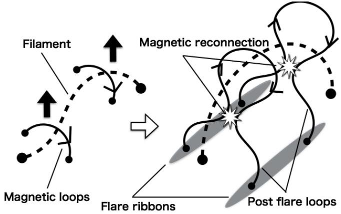

(Kawabata 2016)

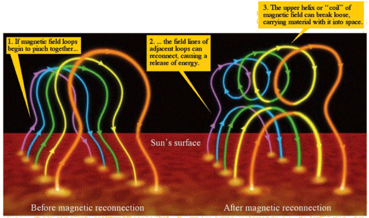

Figure 16-25b
Universe, Eighth Edition

(Freedman & Kaufmann 2008)

A sheared arcade is a 3D counterpart of a CSHKP model.

3D flare models: quadrupolar models

Newly emerging flux tube reconnects with an overlying flux tube, producing two new flux tubes. Both magnetic flux and current partially transferred to new flux tubes.

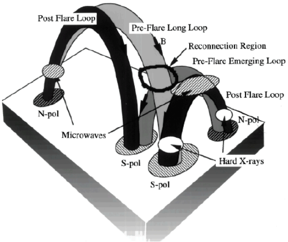

(Nishio et al. 1997)

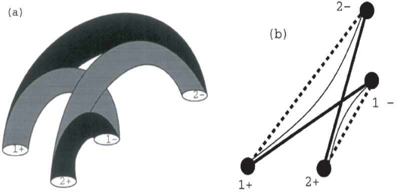

(Melrose 1997)

A model with magnetic flux and current conserved at all four footpoints (Melrose 1997) shows that the change from initial to final magnetic/current configuration releases magnetic energy if the net length of the current path in the corona decreases.

Currents and solar flares

Magnetic free energy <=> large-scale currents

Three classes of currents

1. Currents that close below photosphere
   => potential **B** in corona
2. Currents that close in the corona
   energetically unimportant for a flare
3. Currents that flow through the photosphere at two footpoints

   3a. Currents flowing when flux tube emerges
       close in solar dynamo region

   3b. Currents due to twisting & shearing motion
       close at ↓-propagating Alfvénic front

Only 3a & 3b can store free magnetic energy in corona
(3b cannot provide inferred helicity input)

No counterpart of 3a & 3b on the Earth due to non-conducting atmosphere: only 1 & 2 are possible.

Currents in substorms

Currents before a substorm & reconnection in the magnetotail

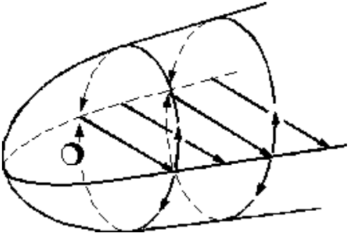

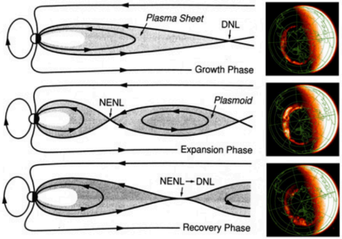

Redirection of current & acceleration resulting in aurorae

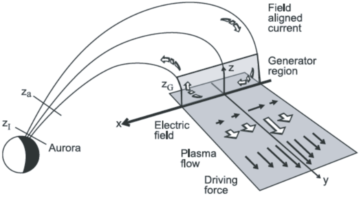

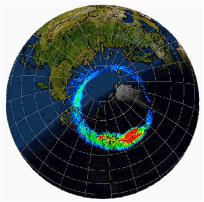

Acceleration region in flares

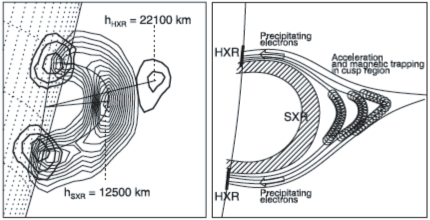

Acceleration during reconnection, or at a shock where outflow stopped by underlying closed field.

Models fail quantitatively: "number problem".

Alternative substorm-like acceleration

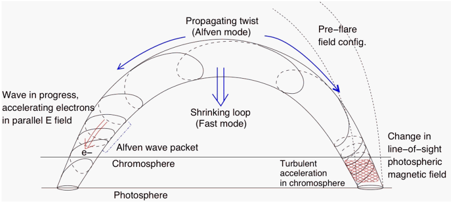

(Fletcher & Hudson 2008)

Magnetic energy released through reconnection goes into kinetic energy in an outflow, and converted to an Alfvénic flux. Acceleration by Alfvén waves near or in chromosphere.

Generation of Alfvénic flux

Energy transport in this model is driven by $\mathbf{E}_\perp$ & $\mathbf{J}_\perp$, and is a Poynting flux due to $\mathbf{E}_\perp$ and the magnetic field generated by $J_\parallel$. How is $J_\parallel$ determined?

$$\mathbf{J}_{\rm tot} = J'_\parallel \mathbf{b} + \mathbf{J}_{\rm pol} + \mathbf{J}_{\rm mag} + \mathbf{J}_{\rm Hall} + \mathbf{J}_{\nabla B} + \mathbf{J}_{\rm curv},$$

$$\mathbf{J}_{\rm mag} = \nabla\times\mathbf{M},\ \mathbf{M} = -(P + \tfrac{1}{2}\eta v^2)\mathbf{b}/B,\ \mathbf{J}_{\rm Hall} = \rho\mathbf{E}_\perp \times \mathbf{b}/B$$

$$\mathbf{B} = B\mathbf{b}, \qquad \mathbf{c} = (\mathbf{b}\cdot\nabla)\mathbf{b} = -\mathbf{b}\times(\nabla\times\mathbf{b}) = \mathbf{n}/R_c,$$

$$\mathbf{J}_\perp = -\frac{\nabla(P + \frac{1}{2}\eta v^2)\times\mathbf{b}}{B} - \frac{\eta v^2}{2B}\mathbf{b}\times\mathbf{c},$$

$$\nabla\cdot\mathbf{J} = 0 \quad => \quad B\frac{\partial}{\partial s}\left(\frac{J_\parallel}{B}\right) = -\nabla\cdot\mathbf{J}_\perp.$$

Integrating gives a modified form of Vasyliunas' formula:

$$\left.\frac{J_\parallel}{B}\right|_{\rm foot} - \left.\frac{J_\parallel}{B}\right|_{\rm apex} = -\mathbf{J}_\perp\cdot\nabla V_B, \qquad V_B = \int\frac{ds}{B}.$$

Currents in solar flares: unneutralized

An isolated flux tube is a misconception.
Coronal currents are unneutralized: no return currents

Like currents attract, opposite currents repel:
current-current forces invoked in earlier solar models

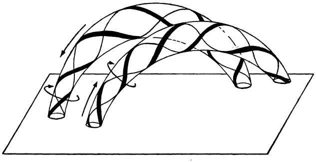

Gold & Hoyle (1960)

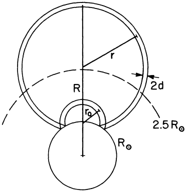

Anzer (1978)

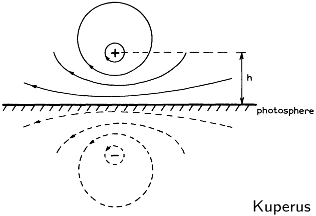

Kuperus & Raadu (1974)

Currents in solar flares: Circuit models

- Circuit models involve neutralized currents
- Driven by postulated photospheric dynamo
- Magnetic energy $\frac{1}{2}LI^2$
- Resistance R shorts direct & return current
- Dissipation due to decrease in I (at fixed L)

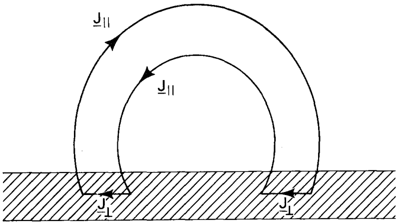

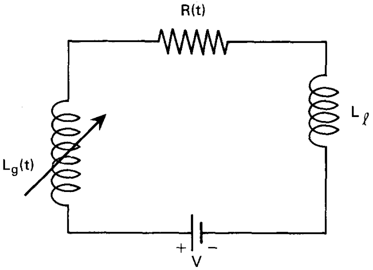

(Spicer 1982)

Circuit models are misleading; not discussed in this talk

Magnetic energy in terms of currents

The total magnetic energy in a volume V is (Jackson 1975)

$$E_{\rm mag} = \frac{1}{2}\int_V d^3\mathbf{x}\,\mathbf{J}(\mathbf{x})\cdot\mathbf{A}(\mathbf{x}), \qquad \mathbf{A}(\mathbf{x}) = \mu_0\int_V d^3\mathbf{x}'\,\frac{\mathbf{J}(\mathbf{x}')}{|\mathbf{x}-\mathbf{x}'|}, \quad (1)$$

$$E_{\rm mag} = \frac{\mu_0}{2}\int_V d^3\mathbf{x}\int_V d^3\mathbf{x}'\,\frac{\mathbf{J}(\mathbf{x})\cdot\mathbf{J}(\mathbf{x}')}{|\mathbf{x}-\mathbf{x}'|} = \int_V d^3\mathbf{x}\,\frac{|\mathbf{B}(\mathbf{x})|^2}{2\mu_0}, \quad (2)$$

where $\mathbf{J}(\mathbf{x})$ is assumed confined to V. Separating into a set of discrete currents , I_i with $i = 1, 2, \ldots$, gives

$$E_{\rm mag} = \tfrac{1}{2}\sum_{ij} M_{ij} I_i I_j = \tfrac{1}{2}\sum_i L_i I_i^2 + \sum_{i<j} M_{ij} I_i I_j, \quad (3)$$

$L_i = M_{ii}$ is self-inductance, M_{ij} for $i \neq j$ is mutual inductance.

Assumption: only coronal contributions to L_i, M_{ij}
can change during a flare.

Current changes during a flare

Model for energy release with unneutralized currents

I_i are fixed by value at solar surface

change in current paths => change in $L_i, M_{ij} \to L'_i, M'_{ij}$

energy available to drive flare if $E'_{\rm mag} < E_{\rm mag}$

Simple models for I_i, M_{ij} used to explore favorable configurations

for maximum energy release (Hardy, Melrose & Hudson 1998)

examples illustrated by (Aschwanden et al. 1999)

energy release at constant L_i possible (Khodachenko et al. 2009)

Qualitatively: energy release when net current path decreases

formation of one long loop tends to be favored

long + short loops — sensitive to orientation of short loop

Need numerical calculations based on force-free magnetic fields

from vector magnetogram data before and after flare

Idealized current-shortening models

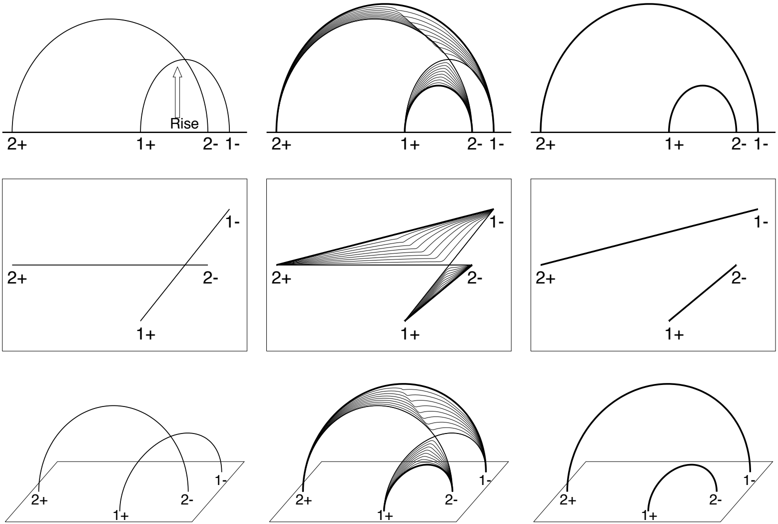

(Aschwanden et al. 1999)

Current lines and magnetic field lines are not distinguished

Magnetic helicity

Magnetic helicity, H, is conserved in a flare:

$$H = \int_V d^3\mathbf{x}\,\mathbf{B}(\mathbf{x}) \cdot \mathbf{A}(\mathbf{x}) = \mu_0 \int_V d^3\mathbf{x} \int_V d^3\mathbf{x}' \,\frac{\mathbf{J}(\mathbf{x}) \cdot \mathbf{J}(\mathbf{x}')}{\alpha(\mathbf{x})|\mathbf{x} - \mathbf{x}'|}, \quad (4)$$

for a force-free magnetic field

$$\mathbf{J}(\mathbf{x}) = \frac{\alpha(\mathbf{x})}{\mu_0}\,\mathbf{B}(\mathbf{x}). \quad (5)$$

with $\alpha(\mathbf{x})$ constant along each current line.

H can be expressed in terms of currents.
For discrete currents, I (Melrose 2004) suggested (incorrectly)

$$H = \sum_i \ell_i I_i^2 + \sum_{i<j} 2m_{ij} I_i I_j, \qquad \ell_i = \frac{\mu_0 L_i}{\alpha_i}, \quad m_{ij} = \frac{2\alpha_i \alpha_j \mu_0 M_{ij}}{\alpha_i + \alpha_j}. \quad (6)$$

Reason (6) not tenable (Démoulin, Pariat, Berger 2006) explained below

Conservation of helicity

Self helicity can be written $H = (T + W)\Phi^2_{\mathrm{mag}}$:
T twist about axis of flux tube: W is writhe of axis (Berger & Field 1984)

Illustration of T and $T + W$ (Démouli & Berger 2003)

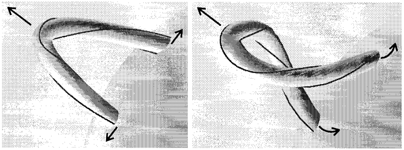

During reconnection only sum $T + W$ is conserved.

Example of mutual helicity (Démoulin, Pariat, Berger 2006)

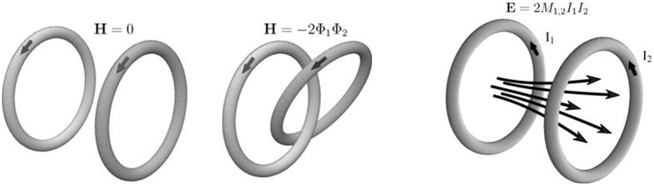

Build up of helicity

Predominantly: $H < 0$ ($H > 0$) in northern (southern) hemisphere

Rising current-carrying flux tubes transport magnetic energy
& helicity into the corona

Estimated $H = 10^{47}\,\mathrm{Mx}^2 \rightarrow$ solar wind per 22-year cycle
$10^{45}\,\mathrm{Mx}^2 \rightarrow$ CMEs (Berger & Ruzmaikin 2000)

Twisting & shearing input too small (van Driel-Gesztelyi, Démoulin & Mandrini 2003)
=> H in emerging current-carrying flux tubes
=> H source in solar dynamo regions

Upper bound on the accumulated helicity (Zhang, Flyer & Low 2006)
Build-up of $H \rightarrow$ upper bound triggers CME?

A possible mechanism for releasing a CME involves threshold for kink instability being exceeded (Török, Kleim & Titov 2004)

Kink instability and CME formation

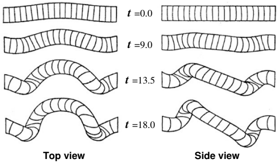

Above: Sakurai (1976).
Right: Fan (2006).

Two illustrations of the development of a kink instability. The instability transforms some twist into writhe.
A simple model for ejection of a CME is when the writhe can form a closed loop, and reconnection allows the plasmoid formed to detatch itself.

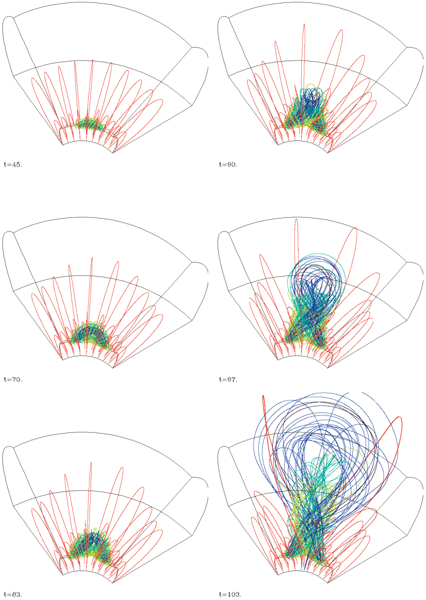

Reconnection in 3D: fan and spine

Expanding the magnetic field around null at $\mathbf{x} = \mathbf{x}_0$ gives

$$B_i = B_{ij}(x_j - x_{0j}) + \cdots, \qquad B_{ij} = (\partial B_i/\partial x_j)_{\mathbf{x}=\mathbf{x}_0}.$$

Regarding B_{ij} as a matrix, $\nabla\cdot\mathbf{B} = 0$ implies that it is traceless, $B_{ii} = 0$. In a 2D null, one of the diagonal components is zero and the other two are equal and opposite. In a 3D null, two of the diagonal components have opposite signs to the third, defining a "fan" plane and a "spine" axis, respectively. A magnetic reconnection model involves two 3D nulls and a null-null line.

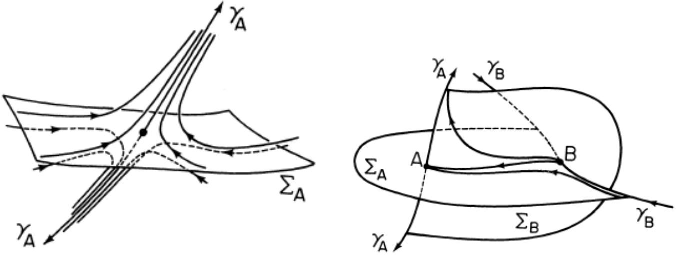

(Lau & Finn, ApJ, **350**, 672, 1990)

Reconnection in 3D: role of currents

Inclusion of current modifies X-point but does not change topological structure (Parnell *et al.* *Phys. Plasmas* **3**, 759, 1996)

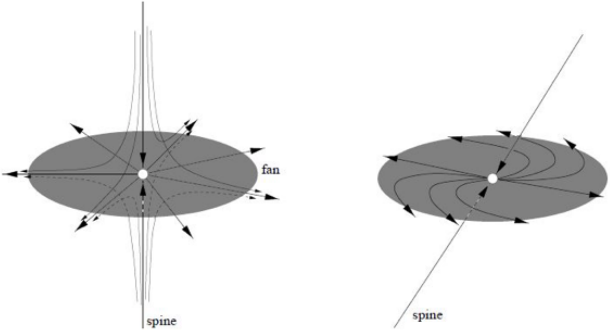

Currents play an essential role in a solar flare, but the relation between these large-scale currents and the currents in individual reconnection regions has not be explored.

Reconnection in 3D: old ideas become new

Separatrices play an important role in 3D reconnection models

(Longcope, *Living Rev. Solar Phys.*, **2**, 2005)

Separatrices identified in quadrupolar models

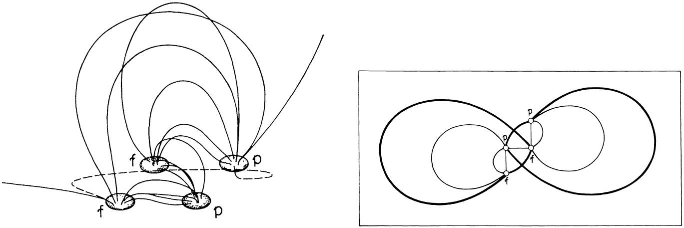

(Baum & Bratenahl, *sol. Phys.* **67**, 245, 1980)

Obvious similarities to early quadrupolar models (Giovanelli 1947; Sweet 1958).

3D reconnection changes large-scale magnetic connectivity,
as in the quadrupolar cartoons (Nishio *et al.* 1997; Melrose 1997).

Early history of reconnection: solar flares

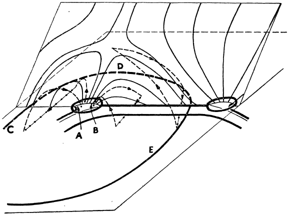

FIG. 1.—*Currents near a growing bipolar spot group.*

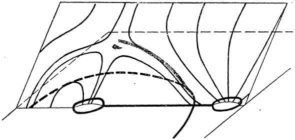

FIG. 2.—*Neutral point flare.*

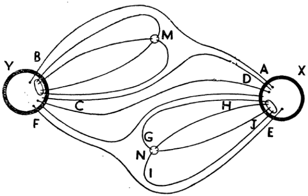

Giovanelli's (1946, 1947, 1948) cartoons for "chromospheric flares" describing currents, magnetic nulls and a quadrupolar magnetic structure, respectively.

Reconnection in 3D: new jargon

A new jargon has developed concerning 3D reconnection, and it is important to recognize this in order to understand the literature.

"Separators" are lines which divide four topologically distinct flux domains (Giovanelli 1947; Sweet 1958; Baum & Bratenahl 1980)

3D magnetic "skeleton" defined by separatrices and null points (Longcope, *Living Rev. Solar Phys.*, **2**, 2005).

3D reconnection in the absence of nulls—new concepts:
- squashing factor Q: gradient in magnetic connectivity
- quasi-separatrix layers (QSLs): regions of anomalously large Q

Projection of magnetic field onto plane perpendicular to separator can be hyperbolic or elliptic

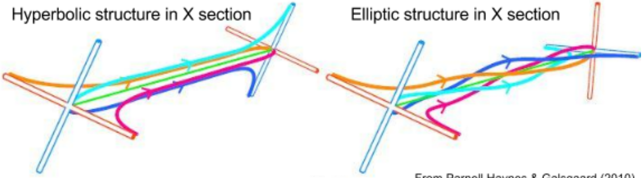

From Parnell,Haynes & Galsgaard (2010)

Reconnection in 3D: applications

These ideas being incorporated into models for solar flares:

Topological model in Jian et al. (2014)

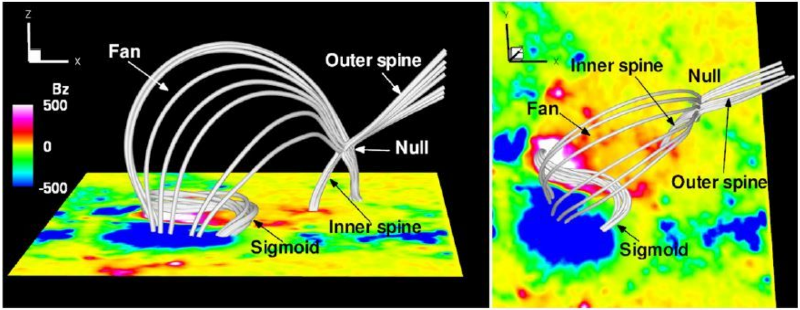

Much more work needs to be done in exploring the implications.

Summary and conclusions

- Magnetic reconnection concept has existed for nearly 70 years
- Early reconnection models were 2D
- Reconnection too slow to explain short timescale of solar flare
- 2D reconnection is potentially misleading:
  some essential effects appear only in 3D
- Anomalous conductivity required; occurs on tiny scale
- Major mismatch ($\sim$ six orders of magnitude) between scale of detailed reconnection models and scale relevant to flares
- Effective dissipation requires a statistically large number of individual reconnection sites
- Large scale structure defined by "skeleton" involving separatrices and nulls
- 3D reconnection in absence of nulls: QSLs, large Q
- Early ideas (Giovanelli 1946–8; Sweet 1958) on nulls, connectivity and currents remain relevant, notably in separatrices and skeletons

Pulsar electrodynamics

Pulsar electrodynamics contains long-standing inconsistencies.

(Melrose & Yuen, *J. Plasma Phys*. **82**, 635820202, 2016)

What determines velocity u of magnetospheric plasma?

Fluid velocity, $\mathbf{u}$, & electric field, $\mathbf{E}$ satisfy: $\mathbf{E} = -\mathbf{u} \times \mathbf{B}$

Does $\mathbf{u}$ determine $\mathbf{E}$, or $\mathbf{E}$ determine $\mathbf{u}$?

Most models get this wrong: electrodynamic problem is to determine $\mathbf{E}$, with $\mathbf{E}$ determining $\mathbf{u}$

Specific global electrodynamic models

- Vacuum dipole model
- Aligned corotation model
- Oblique corotation model
- Force-free electrodynamic models

Vacuum dipole model

Rotating magnetized neutron star in vacuo
dipole axis at **oblique angle**, α, to rotation axis, $\boldsymbol{\omega}$.

Model used to estimate
$B \sin\alpha \propto (P\dot{P})^{1/2}$ & age $P/2\dot{P}$

Intrinsically flawed as stand-alone model

- no plasma $=>$ no pulsar radiation
- slowing down due to magnetic dipole radiation
  incorrect: slowing down due to wind
- magnetic dipole radiation at $\omega = 2\pi/P$ cannot escape
- predicted alignment (Davis & Goldstein 1970),
  $\alpha \to 0$ on spin-down time, not observed

The fields in rotating dipole model can be calculated exactly.
Exact results already applied to magnetic stars (Davis 1947; Deutsch 1955)

Magnetic field

$$\mathbf{B}(t,\mathbf{r}) = \frac{\mu_0}{4\pi}\left[\frac{3\mathbf{r}\,\mathbf{r}\cdot\mathbf{m} - r^2\mathbf{m}}{r^5} + \frac{3\mathbf{r}\,\mathbf{r}\cdot\dot{\mathbf{m}} - r^2\dot{\mathbf{m}}}{r^4 c} + \frac{\mathbf{r}\times(\mathbf{r}\times\ddot{\mathbf{m}})}{r^3 c^2}\right],$$

with $\dot{\mathbf{m}} = \boldsymbol{\omega}\times\mathbf{m}$, $\ddot{\mathbf{m}} = \boldsymbol{\omega}\times(\boldsymbol{\omega}\times\mathbf{m})$.
dipole term $\propto 1/r^3$, inductive term $\propto 1/r^2$, radiative term $\propto 1/r$.

Electric field

$$\mathbf{E}(t,\mathbf{r}) = \frac{\mu_0}{4\pi}\left[\frac{\mathbf{r}\times\dot{\mathbf{m}}}{r^3} + \frac{\mathbf{r}\times\ddot{\mathbf{m}}}{r^2 c}\right],$$

inductive term $\propto 1/r^2$, radiative term $\propto 1/r$.
Radiative terms determine power radiated.

Only terms in red retained in following discussion
others referred to collectively as retarded terms.

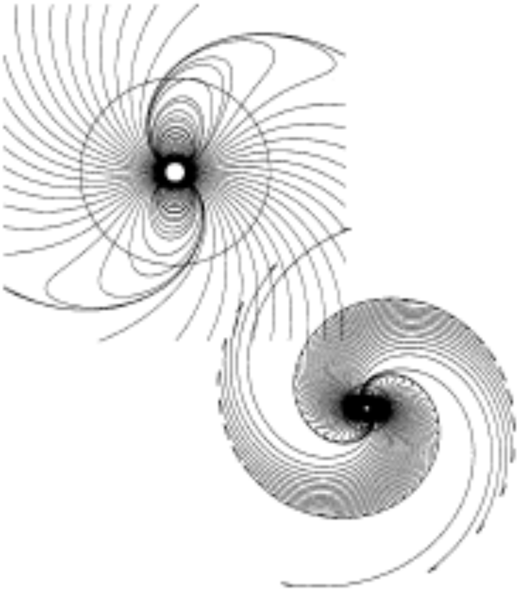

Figure: From Harding (2004)

Corotating models

Plasma assumed to corotate with the star.

$\mathbf{E} = 0$ in corotating frame

$=> \mathbf{E}_{\rm cor} = -(\boldsymbol{\omega} \times \mathbf{r}) \times \mathbf{B}$ in inertial frame.

$=>$ Goldreich-Julian charge density

$\rho_{\rm GJ} = \varepsilon_0 \nabla \cdot \mathbf{E}_{\rm cor} = \varepsilon_0 [-2\boldsymbol{\omega} \cdot \mathbf{B} + (\boldsymbol{\omega} \times \mathbf{r}) \cdot \nabla \times \mathbf{B}]$.

How in neglect of $\mathbf{E}_{\rm ind}$ justified?

The two are comparable:

$$\mathbf{E}_{\rm ind} = \frac{\mu_0 m \omega}{4\pi r^2} \hat{\mathbf{r}} \times (\hat{\boldsymbol{\omega}} \times \hat{\mathbf{m}}), \qquad \mathbf{E}_{\rm cor} = -\frac{\mu_0 m \omega}{4\pi r^2} (3\hat{\boldsymbol{\omega}} \times \hat{\mathbf{r}}\, \hat{\mathbf{r}} \cdot \hat{\mathbf{m}} - \hat{\boldsymbol{\omega}} \times \mathbf{m})$$

Aligned model: $\alpha = 0 => \mathbf{E}_{\rm ind} = 0$ (Goldreich & Julian 1969)

Oblique model: $\mathbf{E}_{\rm ind} = 0$ postulated by assuming

$\nabla \times \mathbf{E} = 0$ in corotating frame (Scharlemann, Arons & Fawley 1978)

Can $\mathbf{E}_{\mathrm{ind}}$ be neglected in oblique rotator?

Electric field can be separated into inductive and potential parts:

$$\mathbf{E} = -\frac{\partial \mathbf{A}}{\partial t} - \nabla\Phi, \qquad \mathbf{E}_{\mathrm{ind}} = -\frac{\partial \mathbf{A}}{\partial t}, \quad \mathbf{E}_{\mathrm{pot}} = -\nabla\Phi.$$

Thought experiment

Start from vacuum model and add plasma.

Charges flow to tend to neutralize $E_{\mathrm{ind}\|} = \mathbf{E}_{\mathrm{ind}} \cdot \mathbf{B}/B$

Complete neutralization requires $E_{\mathrm{ind}\|} + E_{\mathrm{pot}\|} = 0$

Plasma => $\mathbf{E}_{\mathrm{pot}} \neq 0$ but does not change $\mathbf{E}_{\mathrm{ind}}$

$\mathbf{E}_{\mathrm{ind}}$ is always present

Plasma response

Plasma responds to the electric field:

- response to $\mathbf{E}_\perp$ is electric drift: $\mathbf{u} = \mathbf{E}_\perp \times \mathbf{B}/B^2$
- response to $E_\parallel$ is oscillatory at plasma frequency

Electric drift has components due to $\mathbf{E}_{\rm ind}$ and $\mathbf{E}_{\rm pot}$

$$\mathbf{u} = \mathbf{u}_{\rm ind} + \mathbf{u}_{\rm pot}, \qquad \mathbf{u}_{\rm ind} = \frac{\mathbf{E}_{\rm ind} \times \mathbf{B}}{B^2}, \quad \mathbf{u}_{\rm pot} = \frac{\mathbf{E}_{\rm pot} \times \mathbf{B}}{B^2}.$$

If $\mathbf{E} = \mathbf{E}_{\rm cor}$, $\mathbf{u} = \mathbf{u}_{\rm cor\perp}$, $\mathbf{u}_{\rm cor} = \boldsymbol{\omega} \times \mathbf{r}$ => $\mathbf{u}_{\rm pot} = \mathbf{u}_{\rm cor\perp} - \mathbf{u}_{\rm ind}$

Note: magnetosphere of an oblique rotator cannot be corotating
$u_{\rm cor\parallel}$ requires mechanical driver (Hones & Bergeson 1965)
no such driver exists in pulsar magnetosphere

Simple model: (Melrose & Yuen 2013,2014)

$$\mathbf{u} = y\mathbf{u}_{\rm ind} + (1-y)\mathbf{u}_{\rm cor\perp}, \qquad 0 \le y \le 1.$$

=> non-corotational motion parameterized by y.

Gaps in a pulsar magnetosphere

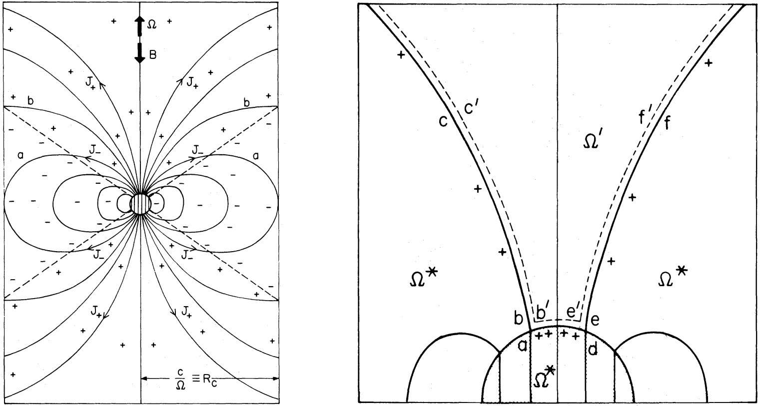

Ruderman & Sutherland, ApJ, **196**, 51 (1975)

Aligned rotator: polar cap defined by the last closed (dipolar) field line and plasma inside the polar cap escapes forming a wind.
Corotation impossible: $\rho \to \infty$ at the light cylinder.
Angular speed changes $\Omega^* \to \Omega'$ across a "gap" with $E_\parallel \neq 0$.

This is a form of generalized reconnection.

Gaps in oblique rotators

Stationary gap models are violently unstable Levinson *et al.* ApJ 631, 456 (2005); Beloborodov & Thompson ApJ 657, 967 (2007)

$E_{\|} \neq 0$ sets up large amplitudes oscillations (LAOs)
Stationary "gaps" replaced by $E_{\|} \neq 0$ in LAOs

Change in $\mathbf{u}_{\rm pot}$ and $\mathbf{E}_{\rm pot} = -\nabla\Phi$ across a gap
due to potential drop $\Phi \to \Phi - \Delta\Phi$ across gap

Detailed model: $\Delta\Phi$ depends on field line constants:
$r_0 = r/\sin^2\theta_b$ and $\phi_0 = \phi_b$

Dependence of $\Delta\Phi(r_0, \phi_0)$ on magnetic azimuthal angle $\phi_0 = \phi_b$
=> dependence on ϕ_b can develop across gap

=> possible model for drifting subpulses
diocotron instability develops in gap
=> dependence on $\cos m\phi_b$

Gaps in FFE models

Force-free electrodynamics (FFE) is related to MHD:
fluid theory with relativistic effects included
and plasma inertia neglected

As in MHD, assumed $E_{\|} = 0 \Rightarrow$ no gaps

FFE models with $E_{\|} = 0$ everywhere lead to singular surfaces
interpreted as current sheets (near light cylinder)
pair creation assumed to occur in these current sheets?

Need for gaps taken into account indirectly in some FFE models

In general, location and distribution of gaps unsolved problem

Is radio source associated with pair creation in a gap?